Microelectronics Reliability 52 (2012) 1441–1444

Contents lists available at SciVerse ScienceDirect

Microelectronics Reliability

journal homepage: www.elsevier.com/locate/microrel

Improved reliability of copper-cored solder joints under a harsh thermal cycling condition

Yunsung Kim [a], Hyelim Choi [a], Hyoungjoo Lee [a], Dongjun Shin [a], Jinhan Cho [b], Heeman Choe [a,*]

[a] School of Advanced Materials Engineering, Kookmin University, Jeongneung-gil 77, Seongbuk-gu, Seoul 136-702, Republic of Korea
[b] Department of Chemical and Biological Engineering, Korea University, Anam-Dong, Seongbuk-gu, Seoul 136-701, Republic of Korea

ARTICLE INFO

Article history:
Received 12 October 2011
Received in revised form 2 March 2012
Accepted 2 March 2012
Available online 28 March 2012

ABSTRACT

This study simulated the performance of Cu-cored solder joints in microelectronic components subjected to the extreme thermal cycling conditions often encountered in the automobile industry by comparing the thermal cycling behavior of Cu-cored solder joints containing two different coating layers of Sn–3.0Ag and Sn–1.0In with that of a baseline Sn–3.0Ag–0.5Cu solder joint under a severe temperature cycling range of −55 to +150 °C. Both Cu-cored solder joints can be considered a potential solution to interconnects in microelectronic semiconductor packages used under harsh thermal conditions on account of their greater resistance to thermal stress caused by the severe temperature cycling than the baseline Sn–3.0Ag–0.5Cu solder joint.

1. Introduction

The health and environmental concerns associated with lead have prompted increasing demand for lead-free solders in the electronic packaging industry, including the popular Sn–Ag–Cu solder [1–7]. Sn–Ag–Cu solder has good potential to replace conventional Sn–Pb solder in many applications owing to its greater strength, thermo-mechanical fatigue behavior and creep resistance at elevated temperatures. Despite its many advantages over conventional Sn–Pb, Sn–Ag–Cu solders often show catastrophic failure under impact loading conditions owing to their much higher stiffness than Sn–Pb solder [8,9]. Moreover, Sn–Ag–Cu solder can show inferior sustainability under harsh conditions, e.g. in microelectronic components subjected to extreme thermal cycling conditions in the automobile industry, because it has a greater dependence on stress at higher stress levels [10,11]. On the other hand, Cu-cored solder balls can be a potential interconnect solution to microelectronic semiconductor packages under harsh thermal conditions, owing to their enhanced reliability for the following reasons. First, Cu-cores in the solder balls can remain in the solid state and serve as a space holder during reflow to prevent the solder balls from touching each other when the ball pitch is fine, as in high-density ball-grid array (BGA) or chip-scale packages (CSPs) [12–16]. Second, their thermal cycling properties are expected to be superior to those of conventional solder because they tend to maintain greater height for the same reason mentioned above and may suffer less stresses, and should also have a lower overall coefficient of thermal expansion (CTE) because of the Cu core inside the ball [13,17]. In spite of all these potential advantages, there have been few reports on the material with the main focus only on its shear strength properties [18,19], except for one thermal cycling study where the thermal cycling resistance of a Cu-cored solder joint increases with increasing size of the Cu-core [20]. Therefore, this study compared the thermal cycling behavior of the Cu-cored solder joint with two different coating layers of Sn–3.0Ag and Sn–1.0In with that of a Sn–Ag–Cu solder joint. The applied thermal cycling range in this study (−55 to +150 °C) is more severe than that experienced in normal cycling (−40 to +125 °C) [21,22] to better simulate the expected reliability of the microelectronic solder joint in the automobile/aerospace industry where harsher operating conditions are being sought to use for better performance; therefore, the result obtained from this study is believed to have useful implications in the automobile and aerospace industries.

2. Experimental procedure

Two types of Cu-cored solder balls (Fukuda Foil & Powder Co., Japan) were examined and compared with the baseline Sn–3.0Ag–0.5Cu solder. Cu-cores, 300 μm in diameter, were electroplated with Sn–3.0Ag or Sn–1.0In solder, resulting in a final uniform diameter of 330 μm. These are hereafter denoted as Sn–3.0Ag Cu-cored and Sn–1.0In Cu-cored solders, respectively. Their thermal cycling properties are examined and compared with that of a commercially available lead-free Sn–3.0Ag–0.5Cu solder (MK Electron, Korea) with the same diameter of 330 μm. The package attachment pads are non-solder mask defined (NSMD) and the

* Corresponding author. Tel.: +82 2 910 4417; fax: +82 2 910 4320.
E-mail address: heeman@kookmin.ac.kr (H. Choe).

0026-2714/$ - see front matter © 2012 Elsevier Ltd. All rights reserved.
http://dx.doi.org/10.1016/j.microrel.2012.03.001

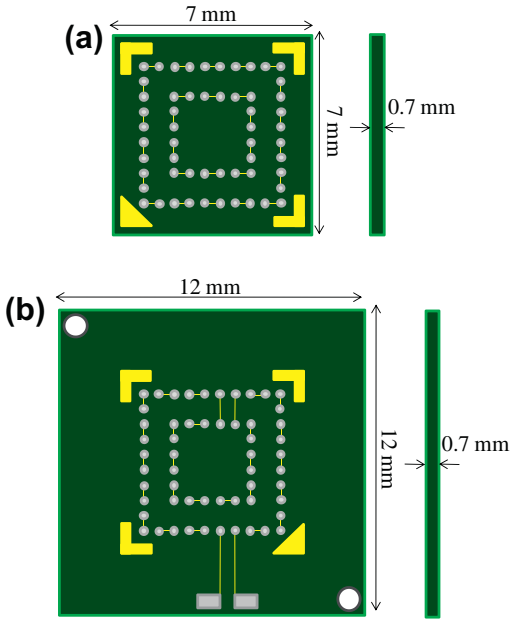

Fig. 1. Schematic diagrams of (a) substrate and (b) board designs with daisy chains.

electrolytic Ni/Au pad finish (of normally used thicknesses of 8–9 μm/0.05–0.07 μm) was applied to all substrates for ball attachment. Both the substrate (7 mm by 7 mm with a thickness of 0.7 mm) and board are FR-4 (12 mm by 12 mm with a thickness of 0.7 mm) with Cu pads of 265 μm diameter. The substrate was designed and connected electrically to a daisy chain, as shown in Fig. 1, to determine the failure of the solder joints in thermal cycling tests. Failure of the solder joint was defined to take place when its electrical resistance was measured to be over ~1 Ω, as accepted also by other studies [21].

The solder balls had been first attached to the substrates in a seven-zone convective reflow oven (1706 EXL, Heller) before they were attached to the boards using Sn–3.0Ag–0.5Cu paste (Heraeusu, German) in a nitrogen atmosphere. The soldering profile had a 150 ± 2 °C preheating temperature with a peak temperature of ~245 °C. The specimens were cycled thermally between −55 °C and +150 °C in air at a frequency of 15 min per cycle until electrical failure. Each test was performed using at least six samples.

3. Results and discussion

Fig. 2 shows the failure rates of Cu-cored solder joints with Sn–3.0Ag and Sn–1.0In plating layers in the thermal fatigue test (−55 to +150 °C, 15 min/cycle) along with that of the baseline SAC305 solder joint for comparison. Three statistically useful parameters are used to carefully make performance comparison between the baseline SAC305, Sn–3.0Ag Cu-cored solder joint, and Sn–1.0In Cu-cored solder joint. First, the mean failure cycles (N_a) for the Sn–3.0Ag and Sn–1.0In Cu-cored solder joints are both higher than that of the SAC305 solder joint (Table 1). Furthermore, both the median failure cycles (N_m) and number of cycles to the first failure (N_0) are also greater for the Sn–3.0Ag and Sn–1.0In Cu-cored solder joints than for the SAC305, which is in consistent agreement with the N_a values (Fig. 2). Of particular interest is the number of cycles to the first failure, N_0, since it can represent the preliminary point of reliability unstability in microelectronic components and be a useful reliability parameter in the industry [21]. The N_0 value of the Sn–3.0Ag Cu-cored solder joint (995 cycles) is the highest, followed by those of the Sn–1.0In Cu-cored solder joint (839 cycles) and SAC305 (324 cycles); both the Cu-cored solder joints show significantly greater resistance to the first failure than the baseline SAC305 solder joint. Despite the tendency of the comparatively rapid failure mechanism after N_0, the Cu-cored solder joints clearly show superior thermal cycling resistance to the SAC305 solder joint with respect to all three parameters of N_a, N_m, and N_0. The similar trend is observed in the two-parameter Weibull plot of Fig. 3, which compares the cumulative failure distributions of the three solder joints using the values of characteristic lifetime, θ and shape factor, β; they represent the number of cycles at 63.2% failure and failure distribution behavior, respectively. The values of θ and β for all three solder joints are displayed in Table 2. Both Sn–3.0Ag and Sn–1.0In Cu-cored solder joints show the higher characteristic lifetime values than the baseline SAC305 solder joint

Table 1
Numbers of thermal fatigue cycles of SAC305 and Cu-cored solder joints until failure: The mean failure cycle number, N_a, median failure cycle number, N_m, and number of cycles to the first failure, N_0.

Failure parameter	Sn–3.0Ag–0.5Cu	Sn–3.0Ag Cu-cored	Sn–1.0In Cu-cored
N_a	1096 ± 742	1526 ± 335	1390 ± 356
N_m	687	1310	1178
N_0	324	995	839

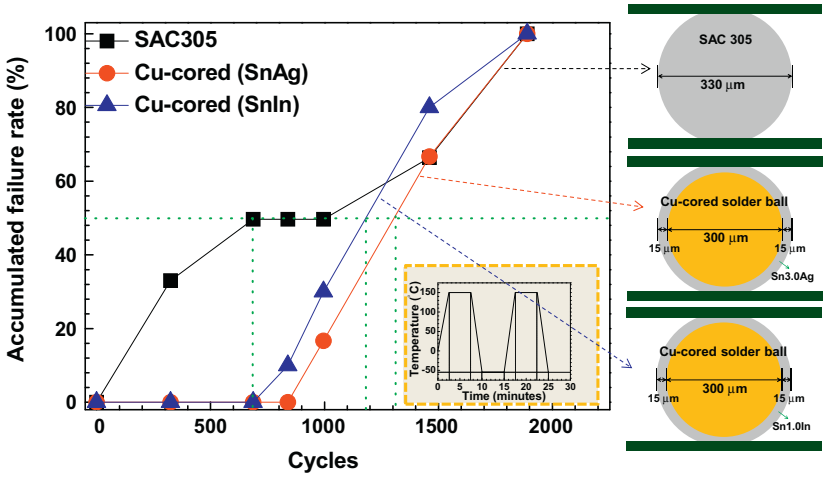

Fig. 2. Failure rates of the Sn–3.0Ag and Sn–1.0In Cu-cored solder joints compared to the SAC305 solder joint during the thermal cycling test. The thermal cycling ranges from −55 to +150 °C, as shown in the inset.

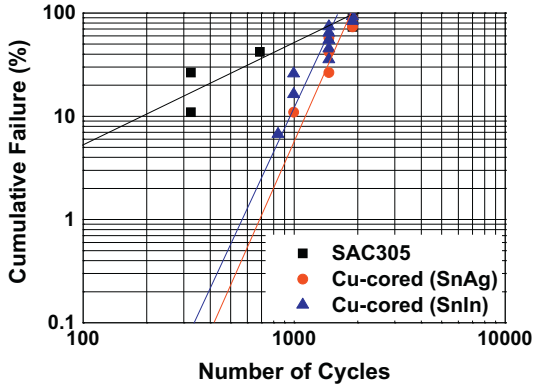

Fig. 3. Weibull distribution of the Sn–3.0Ag and Sn–1.0In Cu-cored solder joints compared to the SAC305 solder joint during the thermal cycling test from −55 to +150 °C.

Table 2
The Weibull characteristic lifetime, θ and shape factor, β for SAC305 and Cu-cored solder joints.

Weibull parameter	Sn–3.0Ag–0.5Cu	Sn–3.0Ag Cu-cored	Sn–1.0In Cu-cored
θ	1444	1690	1563
β	1.2	4.2	3.9

(1444 cycle), with the characteristic lifetime of the Sn–3.0Ag Cu-cored solder joint (1690 cycles) being higher than that of the Sn–1.0In Cu-cored solder joint (1563 cycles). Furthermore, the shape factor, β, is also greater for the Sn–3.0Ag (4.2) and Sn–1.0In (3.9) Cu-cored solder joints than for the baseline SAC305 solder joint (1.2). As a result, the Weibull analysis reveals the superior thermal cycling performance of the Cu-cored solder joints as compared with that of the SAC305 solder joint. This reliability improvement is due to the inherent advantages of the unique Cu-cored solder joint system, consisting of a Cu core and a plating solder layer. Three advantages of the Cu-cored solder joint system may be discussed with regard to its higher thermal cycling reliability: Maintenance of a higher ball height after reflow [10,23,24], the lower CTE of the Cu core, and the lower plastic deformation caused by the thermally cycling stresses owing to the rigid Cu core [23]. First, the mean ball height (376 μm) for the Cu-cored solder joints is approximately 28% higher than the standoff height (293 μm) of the SAC305 solder joint; conversely, the mean solder ball diameter for the Cu-cored solder joints is slightly smaller than that of the SAC305 solder joint after reflow. A greater ball height with a slim ball-shape offers enhanced reliability because the particular geometry can give rise to the lower plastic strain and stress changes during temperature cycling [23,24]. Second, the CTEs of the Cu-cored solder joint systems should be lowered due to the presence of the Cu-core with a comparatively lower CTE (ca. 17 ppm/°C) [23]. Indeed, the CTE of copper is smaller than that of the SAC305 (ca. 23 ppm/°C) [25] and is only slightly higher than that of a printed circuit board (PCB) (ca. 16 ppm/°C) [23]. Therefore, the presence of the Cu-core with the lower CTE value can reduce the average CTE of the entire Cu-cored solder joint system, which might lessen the thermal stress and strain derived from thermal mismatch between the entire solder joint system and PCBs.

In addition, the presence of the Cu-core is anticipated to improve the resistance to electromigration as well, since it acts to reduce the driving force of copper diffusion from the outside to the inside of solder [26]. On the other hand, the presence of the Cu-core may not always be beneficial; the relatively higher stiffness of copper as compared to that of SAC305 solder (131 vs. 48 GPa [8,27]) is expected to result in poorer drop/impact performance [8].

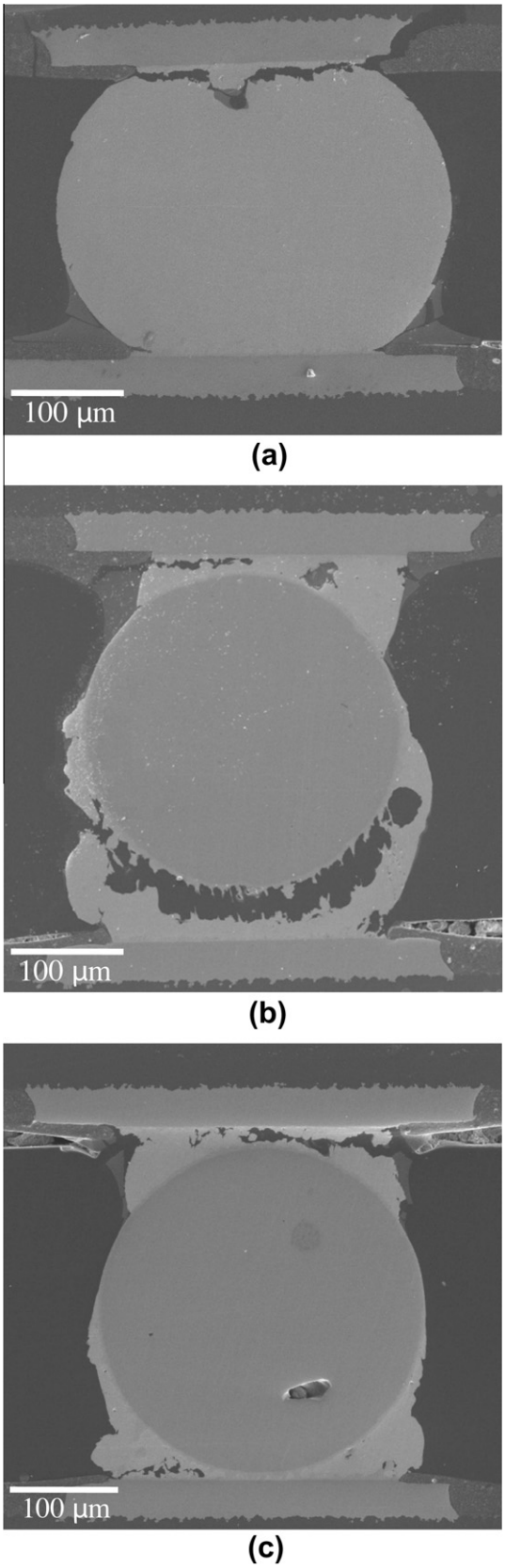

Fig. 4. Scanning electron micrographs of polished cross-sections of (a) SAC305, (b) Cu-cored Sn–3.0Ag and (c) Cu-cored Sn–1.0In solder joints.

Fig. 4 shows cross-sectional scanning electron micrographs of (a) SAC305, (b) Sn–3.0Ag and (c) Sn–1.0In Cu-cored solder joints after thermal cycling failure. Inelastic thermal strain is concentrated in the solder joints where cracks normally initiate and propagate [21,28]. In Fig. 4a, crack propagation takes place near the solder/Cu pad finish interface of the SAC305. This is in agreement with the literature, where the highest stress is concentrated at the interface between the corners of the Cu pad and the solder bulk due to the large CTE mismatch [29–31]. On the other hand, the cross-sectional scanning electron images of the failed Cu-cored solder joints with Sn–3.0Ag and Sn–1.0In plating layers show two different failure modes after the same thermal cycling test. The thermal cycling failure of the Sn–3.0Ag Cu-cored solder joint occurs mostly between the Cu core and plating layer (Fig. 4b), whereas that of the Sn–1.0In Cu-cored solder joint mostly between the plating layer and pad finish (Fig. 4c). One can suppose that the Sn–1.0In Cu-cored solder joint possesses the better wettability characteristic between the Cu-core and Sn–1.0In plating layer than the Sn–3.0Ag Cu-cored solder joint does between the Cu-core and Sn–3.0Ag plating layer, with the interface between the Sn–1.0In plating layer and pad finish thus being the weakest link. This is probably because the addition of indium improves the wettability of solder materials [32,33] by decreasing the wetting time or increasing the wetting force, particularly between the copper and molten Sn-based solder [34,35]. Not only does the composition of the plating alloy affect the thermal cycling performance and failure mechanism, but also the size of Cu-core may have effects on them; it is of interest to refer to a modeling study in which increasing the diameter of Cu-core can lead to increased thermal cycling life [20].

4. Conclusions

The thermal fatigue resistance and fracture mechanisms of Cu-cored solder joints with Sn–3.0Ag and Sn–1.0In plating layers were examined and compared with those of the Sn–3.0Ag–0.5Cu solder joint. The thermal fatigue resistance of the Cu-cored solder joints was improved compared to SAC305 because of the higher ball height maintenance and lower overall CTE caused by the presence of the Cu-core inside the ball, which is also associated with lower degree of plastic deformation strain. Thermal fatigue failure of the Sn–3.0Ag Cu-cored solder joint occurred primarily between the Cu core and plating layer, whereas that of the Sn–1.0In Cu-cored solder joint occurred between the plating layer and pad finish due to the enhanced wettability between the Cu-core and Sn–1.0In plating layer through the addition of indium.

Acknowledgements

This study was supported by the International Research & Development Program of the National Research Foundation of Korea (NRF) funded by the Ministry of Education, Science and Technology (MEST) of Korea. HC also acknowledges the support from the Priority Research Centers Program through the National Research Foundation of Korea (NRF) funded by the Ministry of Education, Science and Technology (2009-0093814; 2010-0029106).

References

[1] Lau YS, Yang PF, Yeh CL. Experimental studies of board-level reliability of chip-scale packages subjected to JEDEC drop test condition. Microelectron Reliab 2006;46:645–50.
[2] Abtew M, Selvaduray G. Lead-free solder in microelectronics. Mater Sci Eng Rep 2000;27:95–141.
[3] Chawla N, Sidhu RS. Microstructure-based modeling of deformation in Pb-free solders. J Mater Sci Mater Electron 2007;18:175–89.
[4] Deng X, Koopman M, Chawla N, Chawla KK. Young's modulus of (Cu, Ag) – Sn intermetallics measured by nanoindentation. Mater Sci Eng A 2004;364:240–3.
[5] Lai YS, Chang HC, Yeh CL. Evaluation of solder joint strengths under ball impact test. Microelectron Reliab 2007;47:2179–87.
[6] Xia Y, Xie X. Endurance of lead-free assembly under board level drop test and thermal cycling. J Alloy Comp 2008;457:198–203.
[7] You T, Kim Y, Jung W, Moon J, Choe H. Effect of surface finish on the fracture behavior of Sn–Ag–Cu solder joints during high-strain rate loading. J Alloys Compd 2009;486:242–5.
[8] You T, Kim Y, Kim J, Lee J, Jung B, Moon J, et al. Predicting the drop performance of solder joints by evaluating the elastic strain energy from high-speed ball pull tests. J Electron Mater 2009;38:410–4.
[9] Choi HL, Lee TK, Kim YS, Kwon H, Tseng CF, Duh JG, et al. Improved strength of boron-doped Sn-1.0Ag-0.5Cu solder joints under aging conditions. Intermetallics 2012;20:155–9.
[10] Liang J, Downes S, Dariavach N, Shangguan D, Heinrich SM. Effects of load and thermal conditions on Pb-free solder joint reliability. J Electron Mater 2004;33:1507–15.
[11] Qi Y, Ghorbani HR, Spelt JK. Thermal fatigue of SnPb and SAC resistor joints: analysis of stress–strain as a function of cycle parameters. IEEE Trans Adv Packag 2006;29:690–700.
[12] Chen CM, Lin HC. Interfacial reactions and mechanical properties of ball-grid-array solder joints using Cu-cored solder balls. J Electron Mater 2006;35:1937–47.
[13] Shohji I, Shiratori Y, Yoshida H, Mizukami M, Ichida A. Growth kinetics of reaction layers in flip chip joints with Cu-cored lead-free solder balls. Mater Trans JIM 2004;45:754–8.
[14] Chiang MJ, Chang SY, Chuang TH. Reflow and burn-in of a Sn–20In–0.8Cu ball grid array package with a Au/Ni/Cu pad. J Electron Mater 2004;33:34–9.
[15] Lee JH, Lim GT, Yang ST, Suh MS, Chung QH, Byun KY, et al. Electromigration and thermomigration characteristics in flip chip Sn–35Ag solder bump. J Kor Inst Met Mater 2008;46:310–4.
[16] Roh MH, Lee HY, Kim WJ, Jung JP. Fabrication and characteristics of electroplated Sn–07Cu micro-bumps for flip-chip packaging. J Kor Inst Met Mater 2011;49:411–8.
[17] Liu P, Yao P, Liu J. Effects of multiple reflows on interfacial reaction and shear strength of SnAgCu and SnPb solder joints with different PCB surface finishes. J Alloys Compd 2009;470:188–94.
[18] Chen CM, Lin HC. Interfacial reactions and mechanical properties of ball-grid-array solder joints using Cu-cored solder balls. J Electron Mater 2006;35:1937–47.
[19] Shohji I, Shiratori Y, Yoshida H, Mizukami M, Ichida A. Growth kinetics of reaction layers in flip chip joints with Cu-cored lead-free solder balls. Mater Trans 2004;45:754–8.
[20] Amagai M, Nakao M. Ball grid array (BGA) packages with the copper core solder balls. In: 48th electronic components and technology conference. 1998. p. 692–701 [May].
[21] Terashima S, Kariya Y, Hosoi T, Tanaka M. Effect of silver content on thermal fatigue life of Sn–xAg–0.5Cu flip–chip interconnects. J Electron Mater 2003;32:1527–33.
[22] Darveaux R, Heckman J, Syed A, Mawer A. Solder joint fatigue life of fine pitch BGAs – impact of design and material choices. Microelectron Reliab 2000;40:1117–27.
[23] Fan XJ, Varia B, Han Q. Design and optimization of thermo-mechanical reliability in wafer level packaging. Microelectron Reliab 2010;50:536–46.
[24] Liu X, Lu GQ. Effects of solder joint shape and height on thermal fatigue lifetime. IEEE Trans Compon Packag Technol 2003;26:455–65.
[25] Nai SML, Wei J, Gupta M. Improving the performance of lead-free solder reinforced with multi-walled carbon nanotubes. Mater Sci Eng A 2006;423:166–9.
[26] Jung DJ, Park DY, Lee JK, Kim HJ, Lee KA. Fabrication and characterization of Cu-based amorphous coatings by cold spray process. J Kor Inst Met Mater 2008;46:321–7.
[27] Chaal L, Debiemme-Chouvy C, Deslouis C, Maurin G, Pailleret A, Saidani B. Comparative AAFM nanoscratching tests in air of bulk copper and electrogenerated cuprous oxide films. Surf Sci 2011;605:121–30.
[28] Lau JH. Flip chip technologies. New York: McGraw-Hill; 1996.
[29] Kim JM, Farson DF, Shin YE. Improvement of board level reliability for μBGA solder joints using underfill. Mater Trans JIM 2003;44:2175–9.
[30] Vandevelde B, Gonzalez M, Limaye P, Ratchev P, Beyne E. Thermal cycling reliability of SnAgCu and SnPb solder joints: a comparison for several IC-packages. Microelectron Reliab 2007;47:259–65.
[31] Terashima S, Tanaka M. Thermal fatigue properties of Sn–1.2Ag–0.5Cu–xNi flip chip interconnects. Mater Trans JIM 2004;45:681–8.
[32] Mei Z, Morris Jr JW. Characterization of eutectic Sn–Bi solder joints. J Electron Mater 1992;21:599–607.
[33] Wang YT, Ho CJ, Tsai HL. Effects of In addition on wetting properties of Sn–Zn–In/Cu soldering. Mater Trans JIM 2010;51:1735–40.
[34] Kanlayasiri K, Mongkolwongrojn M, Ariga T. Influence of indium addition on characteristics of Sn–0.3Ag–0.7Cu solder alloy. J Alloys Compd 2009;485:225–30.
[35] Kim Y, Choi H, Lee H, Shin D, Moon J, Choe H. Fracture behavior of Cu-cored solder joints. J Mater Sci 2011;46:6897–903.